Australian Journal of Basic and Applied Sciences, 7(8): 399-410, 2013
ISSN 1991-8178

Performance Evaluation of Molten Salt Cavity Tubular Solar Central Receiver for Future Integration with Existing Power Plants in Iraq

[1,2]Mahmood S Jamel, [2]A Abd Rahman, [2]A H Shamsuddin

[1]Mechanical Engineering Dept., College of Engineering, University of Basrah, Basrah, Iraq
[2]Centre for Renewable Energy, Universiti Tenaga Nasional, 43000, Kajang, Selangor, Malaysia

Abstract: The performance of the solar central receiver can directly affect the efficiency of the whole power generation system. In this paper an integrated receiver model was developed using MATLAB to evaluate the thermal performance of the solar cavity receiver. It mainly couples heat balance with the temperature computation of receiver walls and the calculation and analysis of the thermal losses. With this model, the thermal performance of a solar cavity receiver is simulated under different environmental conditions ranging from 0 to 50 °C for ambient temperature and 3 to 40 m/s for wind speed. In addition some design parameters like the surface receiver temperature, outlet temperature of molten salt, and receiver absorbed heat were studied and discussed. The results indicated that the parameters of the receiver varied significantly under the sharp disturbance of the receiver aperture area. The wind speed can obviously affect the thermal losses, whose value reaches its maximum at the highest speed. The results were verified with other previous work and good agreement was achieved.

Key words: Solar power tower plant, Central receiver, Molten salt cavity receiver, Heat loss, Thermodynamic performance

INTRODUCTION

The central receiver system (CRS) type of plant depends directly on the type of central receiver while the heliostat fields are almost the same in design although they use different orientation mechanisms. The central receiver, which is typically installed at the top of the solar tower, absorbs solar energy and converts it into thermal energy and has been developed with various shapes, configurations, and working fluids. Volumetric receivers appear to be the best alternative to tube receivers (Ávila-Marín 2011), and have received attention as advanced technology for the deployment of new solar tower power plants due to their advantages from technical and economical viewpoints. But it is still an underdeveloped technology and the superheated steam receiver has poor steam heat transfer capabilities (Kribus, Ries and Spirkl 1996, Buck *et al*. 2006). A cavity tubular receiver with molten salt as the working fluid has the potential to be one of the most cost effective and safe receivers. This type of receiver is divided into two parts: stainless steel tubes and flowing molten salt in the tubes. The receiver efficiency and reliability are the most important factors in the deployment of solar tower power plants.

Many papers have been published in the literature. Hogan *et al.* (Hogan, Diver and Stine 1990) presented a numerical model for solar cavity receivers. Their results showed that both the incident solar power and the convective heat loss coefficient have a strong impact on the receiver thermal performance. Clausing (Clausing 1981) studied the combined convective heat transfer in the cavity receiver and showed that the influences of wind on convective heat loss are fairly minimal. Skycypec *et al.* (Lata, Rodríguez and de Lara 2008) developed the thermal molten salt cavity receiver model and calculated its heat loss, efficiency, and surface temperature at global (entire receiver) and local scales. Li *et al.* (Li *et al*. 2010) established a global steady-state thermal model for a cavity receiver, and studied many factors that influence the receiver performance including the receiver area, emissivity, reflectivity, tube number in the receiver panel, and tube diameter. In this paper, a new model to evaluate molten salt cavity tubular solar central receivers was developed using MATLAB and new performance evaluation parameters were studied and discussed.

Computational Methodology:

Due to the need for proven technology for the purpose of integration with existing plants for future plans in Iraq, tube receivers were selected. The analysis here is based on the cavity receiver. In operation, the receiver absorbs the isolation Q_{rec} from the heliostat field and transports part of the energy to the molten salt flowing through it. The rest of the energy is lost to the environment by convective, emissive, reflective, and conductive heat losses and is expressed by the receiver total heat loss $Q_{rec.totloss}$.

Thermal Performance Of Central Receiver:

The performance of the receiver was evaluated based on the energy principle in this paper. The energy balance for the central receiver is:

Corresponding Authors: Mahmood S Jamel, Mechanical Engineering Dept., College of Engineering, University of Basrah, Basrah, Iraq.
E-mail: mahmood_shaker2005@yahoo.co.uk

$$Q_{rec} = Q_{rec.abs} + Q_{rec.totloss}$$

where $Q_{rec.abs}$ is the receiver absorbed heat. This parameter is taken as a design point for the receiver and is used to calculate the mass flow rate of molten salt. Here, the calculation considers a fixed output temperature operation mode, in which the surface temperature is more stable and the receiver is safer (Li *et al*. 2010), and therefore it is necessary to calculate the proper mass flow rate for molten salt by using the equation:

$$Q_{rec.abs} = m_{ms} Cp_{ms} (T_{ms.o} - T_{ms.i})$$

where m_{ms} is the molten salt mass flow rate in kilograms per second. Then, the energy efficiency of the central receiver subsystem is defined as:

$$\eta_{rec} = \frac{Q_{rec.abs}}{Q_{rec}}$$

Calculation Of Receiver Total Heat Loss:

A modified thermal model for the molten salt cavity receiver is used here to calculate the total heat loss from the central receiver, $Q_{rec.totloss}$, which is based on a validated thermal model developed by (Li *et al*. 2010):

$$Q_{rec.totloss} = Q_{rec.conv} + Q_{rec.em} + Q_{rec.ref} + Q_{rec.con}$$

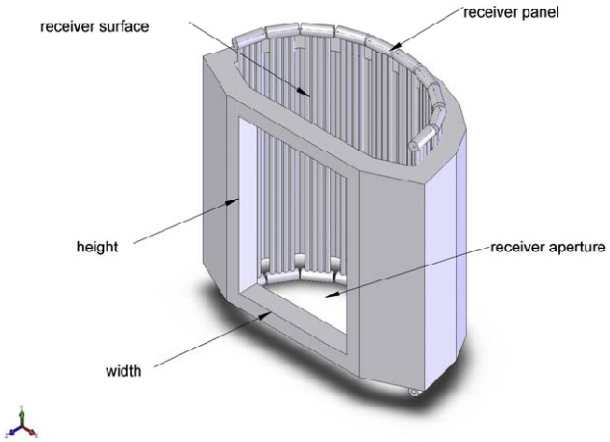

Fig. 1: Schematic diagram of the receiver

The first step in the calculation of heat losses is to calculate the receiver surface temperature, as all types of heat loss are affected by it (except for reflective heat loss). The receiver surface temperature $T_{rec.sur}$ is given by:

$$T_{rec.sur} = \frac{Q_{rec}}{A_{rec.sur}} \left(\frac{d_o}{d_i h_{ms}} + \frac{d_o}{2k_{tube}} \ln \frac{d_o}{d_i} \right) + T_{ms}$$

where T_{ms} is the mean molten salt temperature in the absorber tube. The selected tube material is 316 stainless steel with a conductivity of k_{tube} = 23.9 W/m.K, and the molten salt convective heat transfer coefficient in the absorber tube, h_{ms}, is calculated using the classical Dittus–Boelter equation:

$$h_{ms} = \frac{k_{ms}}{d_i} 0.023 Re_{ms}^{0.8} Pr_{ms}^{0.4}$$

where d_i is the characteristic length and T_{ms} is the characteristic temperature.

The Receiver Emissive Heat Loss:

The emissive heat loss was calculated based on the average receiver surface temperature and expressed by:

$$Q_{rec.em} = \varepsilon_{agv} \sigma (T_{rec.sur}^4 - T_a^4) A_{rec.sur}$$

where the average emissivity, ε_{agv}, is given by:

$$\varepsilon_{agv} = \frac{\varepsilon_w}{\varepsilon_w + (1-\varepsilon_w)F_r}$$

Receiver Convection Losses:

Forced convective heat loss was considered as forced convection from a flat plate (Siebers *et al*. 1984), where the receiver area has the average temperature of the receiver surface, and the forced convective heat losses can be expressed by the equation:

$$Q_{rec.conv.fc} = h_{air.fc.insi}(T_{rec.sur} - T_a)A_{rec.sur}$$

The forced convective heat transfer coefficient is calculated by:

$$h_{air.fc.insi} = \frac{k_{air}}{L} 0.0287 Re_{air.insi}^{0.8} Pr_{air.isni}^{1/3}$$

where L is the reference length, and the reference temperature, $T_{air.insi}$, is the mean temperature between the receiver surface temperature and the ambient temperature. The natural convection heat losses are given by:

$$Q_{rec.conv.nc} = h_{air.nc.insi}(T_{rec.sur} - T_a)A_{rec.sur}$$

The natural convective heat transfer coefficient can be expressed by:

$$h_{air.nc.insi} = 0.81(T_{rec.sur} - T_a)^{0.426}$$

Then the receiver convection losses are:

$$Q_{rec.conv} = Q_{rec.conv.fc} + Q_{rec.conv.nc}$$

The Reflective Heat Loss:

A simple form of the reflective heat loss was used, considering the surface reflectivity and view factor only, and is expressed by:

$$Q_{rec.ref} = Q_{rec}.F_r.R_{rec.sur}$$

where F_r is the view factor and is the ratio between the aperture area and the receiver surface area and can be expressed as:

$$F_r = \frac{A_{ape}}{A_{rec.sur}}$$

The Conductive Heat Loss:

Only conduction from the insulation layer was considered, and it is expressed by the equation:

$$Q_{rec.con} = h_{air.o}(T_{insu.w} - T_a)A_{rec.sur} = \frac{k_{insu}}{\delta_{insu}}(T_{rec.sur} - T_{insu.w})A_{rec.sur}$$

where the combined convective heat transfer is taken into account in calculating the heat transfer coefficient of the outer receiver insulation layer and is given by:

$$h_{air.o} = (h_{air.nc.o}^n + h_{air.fc.o}^n)^{1/n}$$

where n = 1. The natural and forced convective heat transfer coefficient can be expressed by the equations:

$$h_{air.nc.o} = 1.24(T_{insu.w} - T_a)^{1/3}$$

$$h_{air.fc.o} = \frac{k_{air}}{L} 0.0239 Re_{air.o}^{0.805} (0.785\, T_{insu.w}/T_a)^{0.2} 1.167 Pr_{air.o}^{0.45}$$

where L is the reference length, and the reference temperature, $T_{air.insi.w}$, is expressed by

$$T_{air.insi.w} = \frac{T_{insu.w}+T_a}{2}$$

where $T_{insu.w}$ is the insulation wall temperature and is calculated iteratively by the program.

RESULTS AND DISCUSSION

Results Validation:

The evaluation criteria for suggesting plant modification in the present analysis are based on the energy balance. The analysis for the central receiver is based on a thermal model, which is modified from a validated model developed by Li *et al*. (Li *et al*. 2010) and Xu *et al*. (Xu *et al*. 2011). To validate the modification, the present model was used to calculate the thermal performance of the Sandia National Laboratories' molten salt electric experiment (MSEE) based on the parameters provided in Ref. (Li *et al*. 2010). The calculated energy efficiency of the receiver is 86.66%, which gives acceptable agreement with Refs. (Xu *et al*. 2011, Li *et al*. 2010). Meanwhile for the heliostat field subsystem, the calculated efficiencies agree with the results shown in Ref. (Yao *et al*. 2009), and therefore the paper's results are reasonable and useful for guiding the design and integration of CSR.

To evaluate the receiver system, three performance parameters were selected: receiver efficiency, thermal heat losses, and receiver mean surface temperature. Table 1 shows the selected properties of the base case central receiver parameters.

Effect Of Ambient Temperature:

As the focus in the current study is on the possible use of this type of CSR in Basra, Iraq, the Iraqi climatic conditions were selected for this purpose. The selected ambient temperature range is from 0 to 50 °C. In general, there is a little impact of ambient temperature on the selected performance factors of the receiver. Figure 2 shows the effect of the ambient temperature on the receiver mean surface temperature, where the receiver surface

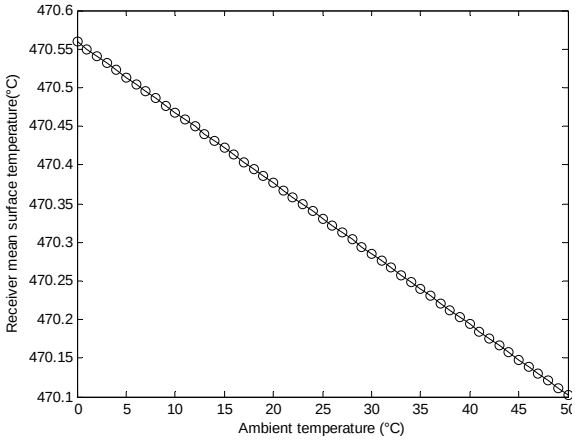

Fig. 2: Effect of the ambient temperature on the receiver mean surface temperature.

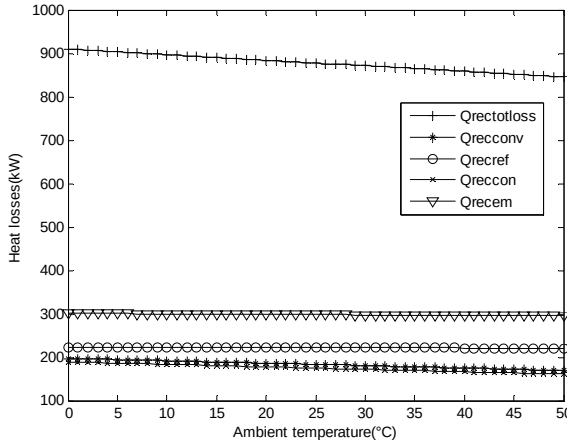

Fig. 3: Effect of the ambient temperature on different types of receiver heat losses and total heat losses.

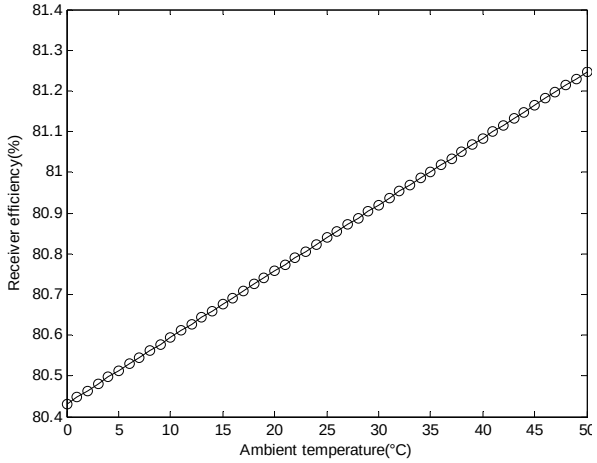

Fig. 4: Effect of the ambient temperature on the receiver efficiency

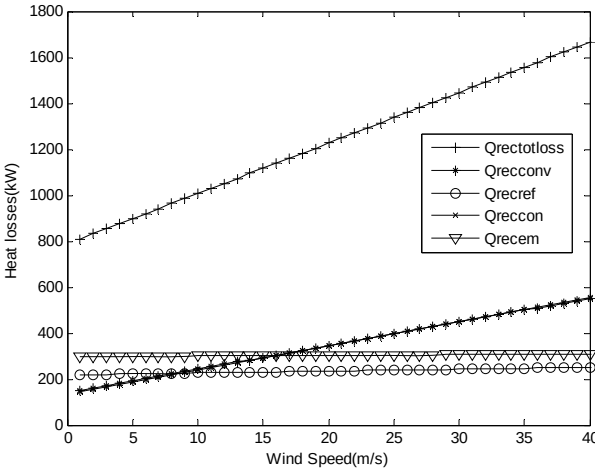

Fig. 5: Effect of changing wind speed on different types of receiver heat losses and total heat losses.

temperature remains almost constant or has a very slight increase with increases in the ambient temperature in the stated range. While the total heat losses decrease slightly from 900 to 850 kW with increasing ambient temperature, as shown in Fig. 3, this is due to a reduction in the temperature difference between the inside of the receiver and the ambient, which leads to a decrease in all types of heat losses, which are affected by the ambient temperature, except for reflective heat losses, which are affected by the incident solar flux. Due to this decrease in total heat losses, there is a small increase in receiver efficiency from 80.4 to 81.2% with increases in the ambient temperature in the stated range, as plotted in Fig. 4.

Effect Of Wind Speed:

In order to investigate the impact of wind conditions on the thermal loss of the receiver, the results are plotted in Fig. 5, which shows the effect of wind speed on different types of thermal losses. It is clear that the total thermal losses increase greatly with increasing wind speed. The wind speeds studied in this work are in the range of 3 to 40 m/s, which represents the Iraqi climatic conditions; these data were collected from the meteorological station located in Basra International Airport. The convective heat losses have the highest percentage of the total heat losses (Li *et al*. 2010).

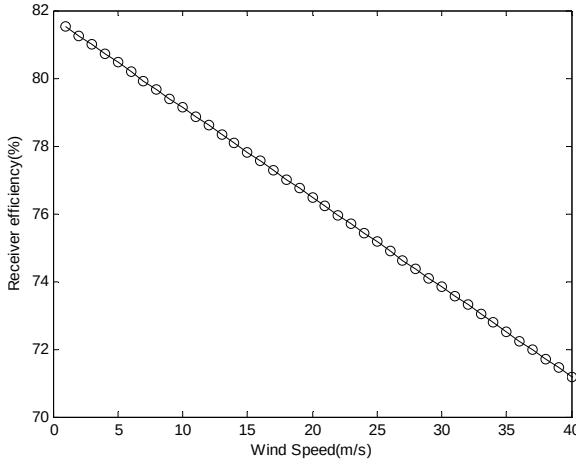

Fig. 6: Effect of changing wind speed on the receiver efficiency.

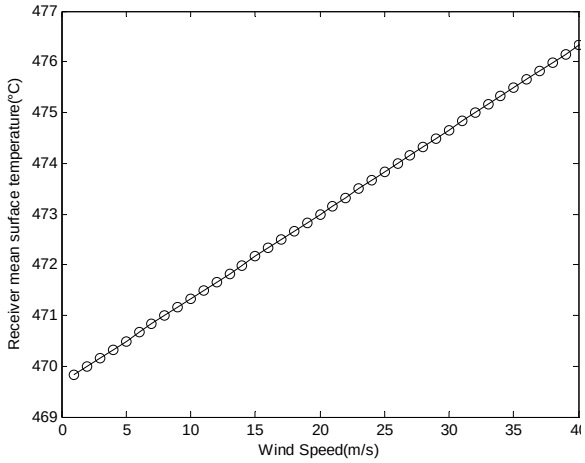

Fig. 7: Effect of changing wind speed on the receiver mean surface temperature.

Table 1: Properties of the base case central receiver parameters

Property	Value unit
The receiver absorbed heat	5600 kW
Receiver area	21.2 m^2
Ambient temperature	25 °C
Inlet temperature of molten salt	290 °C
Outlet temperature of molten salt	560 °C
View factor	0.8
Inlet tube diameter	0.019 m
Inlet tube diameter	0.0223 m
Wall surface emissivity	0.8
Aperture height	6 m
Receiver surface reflectivity	0.04
Conductivity of tube material	19.7 W/mK
Conductivity of insulation	40 W/mK
Insulation layer thickness	0.07
Wind speed	5.0 m/s

From Fig. 5 it can be seen that there is a sharp increase from 150 to 550 kW for the stated range of wind speeds, while all other losses remain almost constant. As a result, the higher wind velocity leads to increasing convective loss and thus total heat losses. As there is a sharp increase in the total heat losses due to an increase in the wind speed then it is logical to see some decrease in receiver efficiency from 82.5 to 71%, as plotted in Fig. 6. In addition, Fig. 7 shows that there is a slight increase in receiver surface temperature from 470 to 476 °C with increasing wind speed for the stated range.

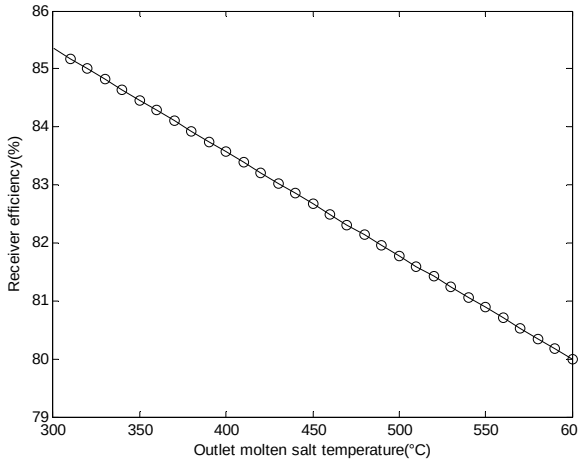

Fig. 8: Effect of changing the outlet molten salt temperature on receiver efficiency.

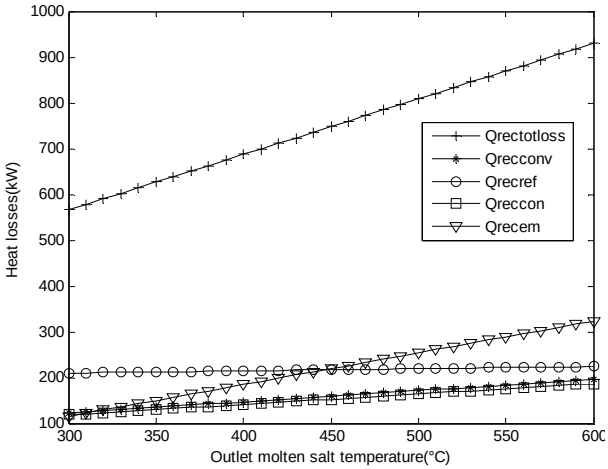

Fig. 9: The relation between outlet molten salt temperature and different types of receiver heat losses

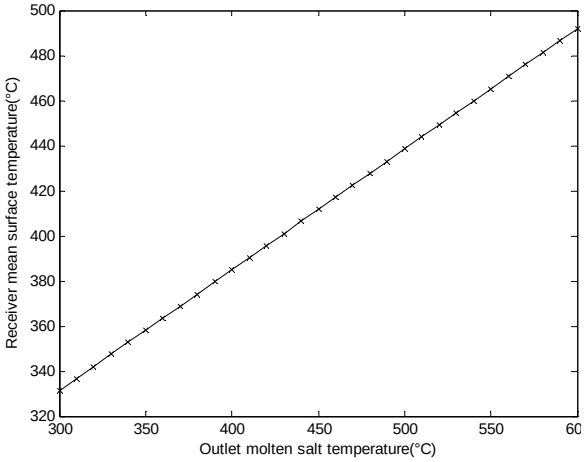

Fig. 10: The relation between outlet molten salt temperature and receiver mean surface temperature.

Effect Of Molten Salt Temperature:

There is some limitation on increasing the outlet temperature of molten salt due to material constraints of the pipes and engine. Anyhow, Fig. 8 shows the variation in the receiver efficiency when the outlet temperature is increased from 300 to 600 °C. It is seen that with the increase in the outlet temperature the efficiency decreased from 85.4 to 80%, which is due to the larger heat loss associated with higher receiver temperature, as

clearly shown in Figs. 9 and 10 . Therefore, efforts must be concentrated on lowering the heat loss, which becomes much trickier at higher working temperatures.

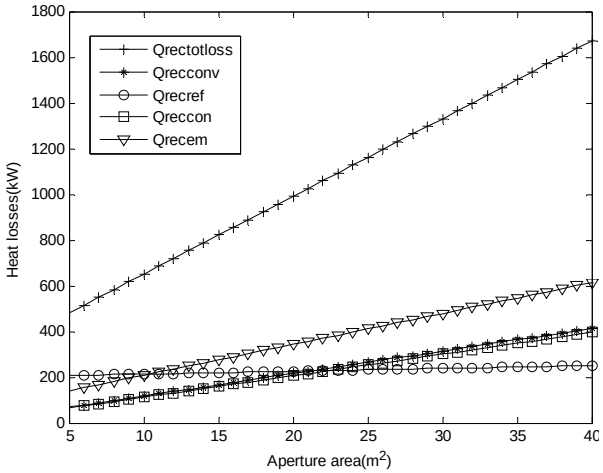

Fig. 11: Effect of changing the aperture area on different types of receiver heat losses and total heat losses.

The Influence Of Receiver Aperture Area:

The larger receiver aperture area produced greater total heat losses, as shown in Fig. 11. When the receiver aperture area increased, all types of heat losses increased except for reflective heat loss, which is a function of incident solar flux. Fig. 12 shows that when the receiver aperture area increased, the receiver surface temperature decreased and the heat loss potentially decreased, but in reality when the receiver area increased, the heat loss also increased due to the increase in the area of heat transfer.

On the other hand, the efficiency was at a maximum and total heat loss was at a minimum at the smallest receiver aperture area, as shown in Fig. 13, because an increase in total heat losses leads to an increase in the receiver efficiency. As a result, the receiver aperture area has a greater influence on the performance parameters of the receiver as there is a very sharp increase in the total heat losses from 500 to 1680 kW for the selected range of receiver aperture areas from 5 to 40 m^2, and this makes a critical path in the receiver design.

Effect Of Receiver Absorbed Heat:

In general, the performance of the central solar power plant is highly dependent on the incident solar isolation, which varies with the geographical position, the time of day, and so on. In this study, the aim is to use the receiver for future integration with existing steam power plants, and therefore there is needing to explore how $Q_{rec.abs}$ affects the receiver performance.

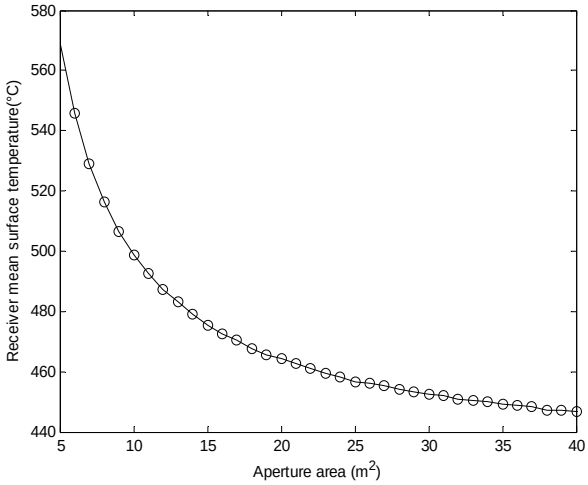

Fig. 12: The relation between aperture area and receiver mean surface temperature.

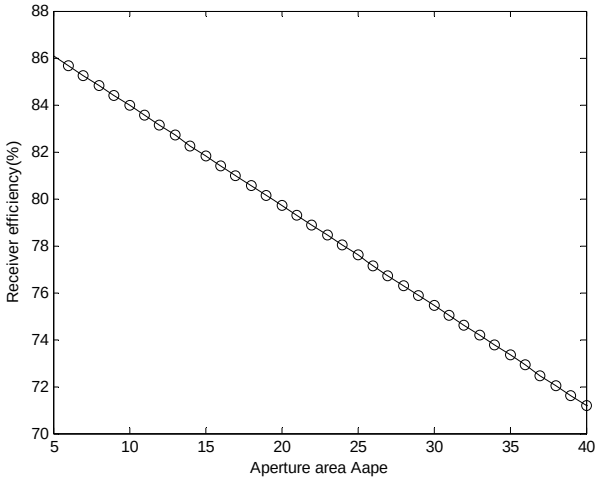

Fig. 13: Effect of changing aperture area on receiver efficiency.

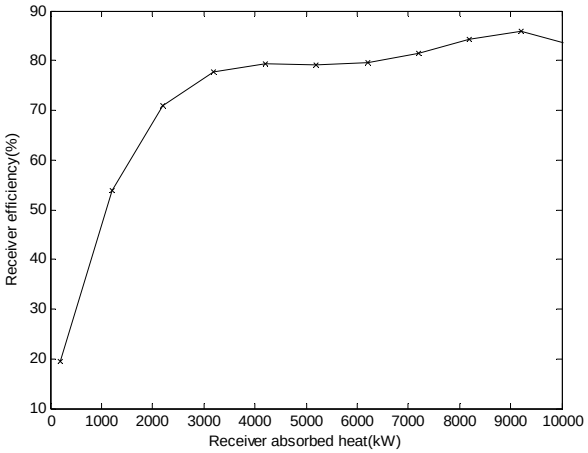

Fig. 14: Effect of changing the receiver absorbed heat on receiver efficiency.

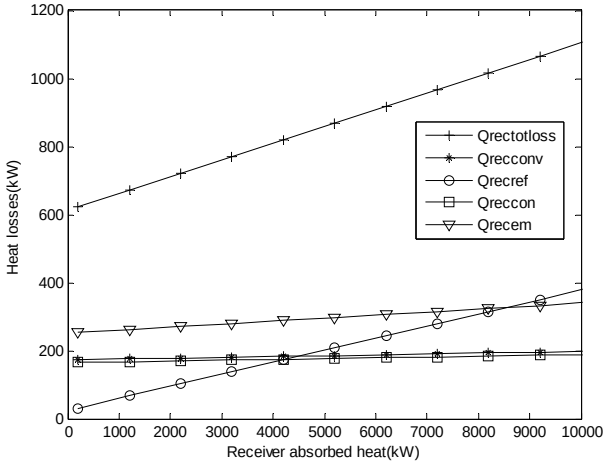

Fig. 15: Effect of changing the receiver absorbed heat on different types of receiver heat losses.

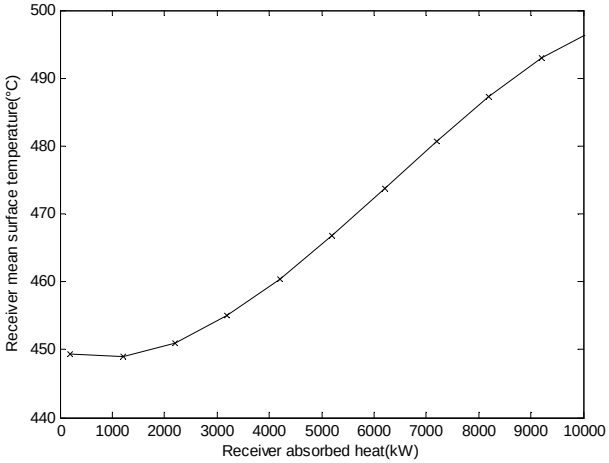

Fig. 16: The relation between receiver absorbed heat and receiver mean surface temperature.

Table 2: The effect of selected performance parameters on receiver efficiency and total heat losses.

	Receiver efficiency (%)	Total heat losses (kW)
Ambient temperature	80.4 to 81.2	900 to 850
Wind speed	81.4 to 71.5	800 to 1680
Outlet temperature of molten salt	85.4 to 80	570 to 940
Aperture area	86 to 71.5	500 to 1680
Receiver absorbed heat	20 to 85	600 to 1100

The $Q_{rec.abs}$ is taken here as a design point for the receiver and is used to calculate the mass flow rate of molten salt. To investigate the effect of this parameter, different design values ranging from 100 to 10000 kW were tested in this work. Figure 14 shows the variation in the receiver efficiency as a function of $Q_{rec.abs}$. It is seen that receiver efficiency increases with the increase in $Q_{rec.abs}$. The increase in efficiency of the receiver with $Q_{rec.abs}$ can be explained by analysing the heat loss mechanism from the receiver as shown in Fig. 15. There are three types of heat losses, namely emissive heat loss, convective heat loss, and conductive heat loss, which depend mainly on the surface temperature of the receiver $T_{rec.sur}$. The change in $T_{rec.sur}$ of the receiver with $Q_{rec.abs}$ can be seen in Fig. 16, which shows clearly that when $Q_{rec.abs}$ increases from 100 to 10000 kW the receiver surface temperature varies only slightly, from 450 to 495 °C, and as a result the heat loss from the receiver increases only slightly when the input energy increases proportionally, which results in an increase in the receiver efficiency with $Q_{rec.abs}$. In addition, it should be pointed out that in Fig. 16 $T_{rec.sur}$ decreases slightly first at low values of $Q_{rec.abs}$, in the range below 2000 kW. This is due to the assumption that the molten salt is always heated from 290 to 565 °C through the receiver. Therefore to maintain a fixed hot molten salt temperature at the receiver outlet, the molten salt flow rate should be very low, carrying less heat away and leaving more heat, which heats up the receiver. It is also seen that there is unsystematic variation in the receiver efficiency effect with $Q_{rec.abs}$. For instance, the energy efficiency of the receiver increases greatly from about 40 to 80% when $Q_{rec.abs}$ increases from 100 to 4000 kW but increases only slightly from 80 to 85% when $Q_{rec.abs}$ increases further from 4000 to 10000 kW.

With regard to environmental factors, namely wind speed and ambient temperature, wind speed has a greater impact on receiver efficiency and total heat losses than ambient temperature as there are very sharp increases in total heat losses from 800 to 1680 kW in the wind speed range from 3 to 4 m/s while there is a very slight decrease for ambient temperature. With regard to design factors including the outlet temperature of molten salt, aperture area, and receiver absorbed heat, the receiver aperture area has the greatest influence on total heat losses, with a slight decrease in receiver efficiency from 86 to 71.5% in the aperture area range from 3 to 40 m^2. Moreover the receiver absorbed heat has a very sharp increase in receiver efficiency from 20 to 85% with moderate total heat losses from 600 to 1100 kW for the tested range of values of receiver absorbed heat. In this situation, the receiver aperture area and absorbed heat should be tested until the optimal design is achieved.

Conclusion:

New environmental and design parameters are studied in this paper through an integrated receiver model. This model evaluated the thermal performance of a molten salt solar cavity receiver. An ambient temperature range of 0 to 50 °C and a wind speed range of 3 to 40 m/s were studied and discussed, in addition to some design parameters like surface receiver temperature, outlet temperature of molten salt, and receiver absorbed heat. The results indicated that wind speed has a greater impact on the receiver performance parameters than the ambient temperature. Also, the receiver aperture area has a large influence on total heat losses and receiver

efficiency. Meanwhile the receiver absorbed heat has a very sharp increase in receiver efficiency with moderate total heat losses for the tested range of values of receiver absorbed heat. Under this condition, the designer should select the lowest wind speed site along with the optimal design that matches the receiver aperture area with the absorbed heat.

Appendix A:

Air properties equations as a function of temperature (Reid 1966):

Density (kg/m^3): $\rho_{air} = \frac{351.99}{T_{air}} + \frac{344.84}{{T_{air}}^2}$

Specific heat for air (J/kg K): $C_{P_{air}} = 1030.5 - 0.19975T_{air} + 3.9734 * 10^{-4}{T_{air}}^2$

Thermal conductivity for air (W/mK): $k_{air} = \frac{2.334*10^{-3}{T_{air}}^{3/2}}{164.54+T_{air}}$

Absolute viscosity for air (N S/m^2): $\mu_{air} = \left(\frac{1.4592{T_{air}}^{3/2}}{109.1+T_{air}}\right) \times 10^{-6}$

The properties of molten salt as a function of temperature (i.e., a mixture of 60 wt% NaNO3 and 40 wt% KNO3) are (Zavoico 2001):

Density of molten salt (kg/m^3): $\rho_{ms} = 2090 - 0.636T_{ms}(°C)$

Specific heat for molten salt (J/kg K) : $C_{P_{ms}} = 1443 + 0.172T_{ms}(°C)$

Thermal conductivity for molten salt (W/mK) $k_{ms} = 0.443 + 1.9 \times 10^{-4}T_{ms}(°C)$

Absolute viscosity (N S/m^2): $\mu_{ms} = \left(22.714 - 0.12\,T_{ms}(°C) + 2.281 \times 10^{-4}T_{ms}^2(°C) - 1.474 \times 10^{-7}T_{ms}^3(°C)\right) \times 10^{-6}$

Nomenclature		Subscript	
A	Area(m^2)	a	Ambient
Cp	Specific heat at constant pressure (W/m^2.K)	air	Air
d	Diameter (m)	abs	Absorbed energy
F_r	View factor	avg	Average
H	Heat transfer coefficient(W/m^2.K)	con	Conductive heat loss
K	Conductivity (W/m.K)	conv	Convective heat loss
Q	Heat (kW)	em	Emissive heat loss
T	Temperature (°C)	fc	Forced convection
Re	Reynolds number	i	Inner tube or inlet
Pr	Prandtle number	isni	Inner side of receiver
M	Mass flow rate (kg/s)	insu	Insulation
L	Aperture height (m)	loss	Heat loss
R	Reflectivity	ms	Molten salt
Greek symbols		nc	Natural convection
η	Efficiency	o	Outer tube or outlet
ε	Emissivity	rec	Receiver
σ	Stefan–Boltzmann constant 5.67 × 10^{-8} (W/m^2.K^4)	ref	Reflective heat loss
μ	Dynamic viscosity(N S/m^2)	sur	Surface
ρ	Density (kg/m^3)	tube	Receiver absorber tube
δ	Insulation thickness	total	Total heat loss
		w	Wall surface

REFERENCES

Ávila-Marín, A.L., 2011. Volumetric receivers in Solar Thermal Power Plants with Central Receiver System technology: A review. *Solar Energy,* 85: 891-910.

Buck, R., C. Barth, M. Eck & W.-D. Steinmann, 2006. Dual-receiver concept for solar towers. *Solar Energy,* 80: 1249-1254.

Clausing, A.M., 1981. An analysis of convective losses from cavity solar central receivers. *Solar Energy,* 27: 295-300.

Hogan, R.E., R.B. Diver & W.B. Stine, 1990. Comparison of a Cavity Solar Receiver Numerical Model and Experimental Data. *Journal of Solar Energy Engineering,* 112: 183-190.

Kribus, A., H. Ries & W. Spirkl, 1996. Inherent Limitations of Volumetric Solar Receivers. *Journal of Solar Energy Engineering,* 118: 151-155.

Lata, J.M., M. Rodríguez & M.Á. de Lara, 2008. High Flux Central Receivers of Molten Salts for the New Generation of Commercial Stand-Alone Solar Power Plants. *Journal of Solar Energy Engineering,* 130: 021002-021002.

Li, X., W. Kong, Z. Wang, C. Chang & F. Bai, 2010. Thermal model and thermodynamic performance of molten salt cavity receiver. *Renewable Energy,* 35: 981-988.

Reid, R.C., Sherwood, K. Thomas, 1966. *The Properties of Gases and Liquids*. McGraw-Hill.

Siebers, D.L., J.S. Kraabel, S.N. Laboratories & U.S.D.o. Energy, 1984. *Estimating Convective Energy Losses from Solar Central Receivers*. Sandia National Laboratories for the U.S. Department of Energy.

Xu, C., Z. Wang, X. Li & F. Sun, 2011. Energy and exergy analysis of solar power tower plants. *Applied Thermal Engineering,* 31: 3904-3913.

Yao, Z., Z. Wang, Z. Lu & X. Wei, 2009. Modeling and simulation of the pioneer 1MW solar thermal central receiver system in China. *Renewable Energy,* 34: 2437-2446.

Zavoico, A.B., 2001. Solar Power Tower Design Basis Document. Sandia National Laboratories.